

Crystal structure and Mössbauer spectrum of vonsenite, $2\text{FeO} \cdot \text{FeBO}_3$

J. S. SWINNEA AND HUGO STEINFINK

Materials Science Laboratories
Department of Chemical Engineering
The University of Texas, Austin, Texas 78712

Abstract

The crystal structure of the mineral vonsenite has been redetermined from a synthesized specimen of composition $2\text{FeO} \cdot \text{FeBO}_3$. The unit cell dimensions are $a = 9.463(1)\text{Å}$, $b = 12.305(1)\text{Å}$, $c = 3.0727(6)\text{Å}$, $Z = 4$, space group *Pbam*. The final coordinates gave $R = 0.054$ and $\omega R = 0.029$ for 614 structure amplitudes and $R = 0.030$, $\omega R = 0.027$ for 461 amplitudes greater than $2\sigma(F)$. The crystal structure is essentially unchanged from the structure reported in 1950 but the precision of the parameters is at least an order of magnitude better. Values of valence sums, Mössbauer spectra, and the distortions present in the four crystallographically independent octahedra containing Fe1, Fe2, Fe3 and Fe4 are consistent with the presence of two pairs of physically distinct iron ions. Fe1 and Fe3 are divalent; the bond distance between Fe2 and Fe4 is 2.787Å and direct exchange occurs so that an intermediate oxidation state of +2.5 is observed. The Mössbauer spectra are complex and indicate the presence in the structure of Fe^{2+} , Fe^{3+} and $\text{Fe}^{2.5+}$. As the temperature is lowered from room temperature the Mössbauer spectra show the migration of a low velocity peak due to Fe^{3+} towards the high velocity peak due to the dinuclear complex Fe2–Fe4 in which Fe has an intermediate valence state. At room temperature charge delocalization is present over the three-dimensional structure because the next nearest Fe2–Fe2 and Fe4–Fe4 distances of 3.073Å parallel to *c* provide a path. However, as the temperature is lowered this rather large Fe–Fe distance becomes a barrier to delocalization and only the charge transfer between Fe2 and Fe4 remains.

Introduction

The mineral vonsenite is one end member of the series ludwigite-vonsenite in which the composition varies from $2\text{MgO} \cdot \text{FeBO}_3$ for the former to $2\text{FeO} \cdot \text{FeBO}_3$ for the latter. The minerals may contain varying ratios of Mg^{2+} , Mn^{2+} and Fe^{2+} in the divalent site as well as Al and Ti in the ferric ion site. The structures of ludwigite and the related minerals warwickite and pinakiolite were determined by Takéuchi *et al.* (1950) primarily from anion packing considerations. Takéuchi also later published the crystal structure of vonsenite (1956). Bertaut (1950) synthesized a series of boroferrites with the ludwigite, warwickite and pinakiolite structures, in which the divalent sites were occupied by Fe, Co, Ni, Cu and Mg, and the trivalent sites by Fe, Ti^{4+} and Mn. He determined their lattice constants and space groups. An abstract providing preliminary atomic positions and bond lengths for ludwigite was published by Carvalho da Silva *et al.* (1955) but no further work has appeared. Numerous references to these minerals and indexed powder diffraction patterns exist in the literature (Eakle, 1920; Leonard and Vlisidis, 1960, 1961; Ruiz and Salvador, 1971, Franz *et al.*, 1981).

A refinement of the ludwigite structure from a mineral specimen of composition $(\text{Mg}_{1.85}\text{Fe}_{0.15}^{2+})(\text{Fe}_{0.60}\text{Al}_{0.40})\text{BO}_3$

described the distribution of the cations over the four crystallographically independent sites on the basis of electron density peak heights in (001) electron density projections (Mokeyeva, 1968). It was concluded that the M3 octahedral site in ludwigite was preferentially occupied by Fe^{2+} . Malisheva *et al.* (1971) discussed the results obtained from Mössbauer spectra on a series of minerals from the ludwigite-vonsenite series and also postulated that Fe^{2+} , when substituting for Mg, initially “enters first of all the most regular octahedron M3.”

No recent three-dimensional crystal structure determination of the iron end member vonsenite, $2\text{FeO} \cdot \text{FeBO}_3$, with reliable bond lengths exists and we undertook to synthesize this phase, redetermine its structure and investigate its Mössbauer spectrum.

Preparation

The starting materials for the preparation of vonsenite were Fe, Fe_2O_3 and B_2O_3 . The Fe and Fe_2O_3 powders (Alfa Inorganics) were nominally 99.9+ % pure. An X-ray powder diffraction pattern of the B_2O_3 powder (Eastman Kodak) showed no extraneous lines. The stoichiometric mixture $4\text{Fe}:7\text{Fe}_2\text{O}_3:3\text{B}_2\text{O}_3$ was packed into a capped carbon crucible and then sealed in a vycor tube under a

Table 1. Positional parameters and anisotropic thermal vibrations* ($\times 10^4$) for vonsenite

| Atom | x | y | z | β_{11} | β_{22} | β_{33} | β_{12} | β_{13} | β_{23} |
|------|---------|------------|------|--------------|--------------|--------------|--------------|--------------|--------------|
| Fe1 | 0 | 0 | 0 | 12 (1) | 7.7(.6) | 223(12) | -3.3(.8) | 0 | 0 |
| Fe2 | 5000 | 0 | 5000 | 41 (1) | 7.4(.7) | 140(12) | -6.5(8) | 0 | 0 |
| Fe3 | 4(1)** | 2741.6(.6) | 0 | 12.6(.8) | 7.0(.5) | 193(9) | 1.8(.7) | 0 | 0 |
| Fe4 | 7443(1) | 3876.8(.6) | 5000 | 13.3(.8) | 8.9(.4) | 144(7) | 2.3(.5) | 0 | 0 |
| O1 | 8431(4) | 422 (3) | 5000 | 14 (4) | 7 (2) | 277(46) | -2 (3) | 0 | 0 |
| O2 | 3876(4) | 787 (3) | 0 | 15 (4) | 8 (2) | 222(49) | 3 (3) | 0 | 0 |
| O3 | 6227(4) | 1382 (3) | 5000 | 12 (4) | 6 (2) | 276(42) | -4 (3) | 0 | 0 |
| O4 | 1129(4) | 1409 (3) | 0 | 11 (4) | 7 (2) | 261(44) | 1 (3) | 0 | 0 |
| O5 | 8402(5) | 2365 (3) | 5000 | 11 (4) | 9 (2) | 259(48) | -2 (3) | 0 | 0 |
| B | 2683(7) | 3608 (5) | 5000 | 30 (7) | 8 (3) | 119(54) | -7 (5) | 0 | 0 |

* The temperature factor is $\exp[-(\beta_{11}h^2 + \beta_{22}k^2 + \beta_{33}l^2 + 2\beta_{12}hk + 2\beta_{13}hl + 2\beta_{23}kl)]$
** Numbers in parentheses are standard deviations and refer to the last digit.

vacuum of 10^{-3} torr. The mixture was heated at 900°C for three days and then cooled to ambient temperature by turning off power to the furnace. When the vycor tube was opened a loud popping sound was heard, indicating excessive pressure in the tube. This pressurization of the tube was probably due to excess O_2 resulting from incomplete conversion of the starting materials to vonsenite. Indeed, an X-ray powder diffraction pattern of the black product which consisted of aggregates of many needle-like crystals showed that in addition to vonsenite trace amounts of Fe were also present. Any unreacted B_2O_3 in the mixture would not be identifiable because B_2O_3 becomes amorphous upon melting.

X-ray structure determination

An acicular crystal from the reaction product was mounted on a goniometer head and Weissenberg and precession X-ray diffraction pictures indicated a unit cell of $a = 9.5\text{\AA}$, $b = 12.3\text{\AA}$, $c = 3.07\text{\AA}$, space group $Pbam$ or $Pba2$ thus confirming that it was vonsenite. A crystal having dimensions $20 \times 25 \times 345 \mu\text{m}$ was then mounted on a Syntex autodiffractometer equipped with a graphite monochromator and data were collected using $\text{MoK}\alpha$ radiation. A least squares refinement of 30 reflections measured between 25.64° and 29.34° 2θ yielded $a = 9.463(1)\text{\AA}$, $b = 12.305(1)\text{\AA}$, $c = 3.0727(6)\text{\AA}$. Of 615 intensities collected to $2\theta = 60^\circ$ by the variable ω -scan technique at rates from 2.0 to 5.0 deg min^{-1} , 465 $F(hkl)$ were considered observed on the basis of having values exceeding $2\sigma(F)$. The measured intensities were corrected for Lorentz, polarization and absorption effects using $\mu = 121.8 \text{ cm}^{-1}$. The absorption factors ranged from 1.27 to 1.38. Estimated errors of the intensities were calculated from $\sigma(F^2) = [S^2(I_p + 1/R^2(I_{B_1} + I_{B_2})) + (pI_{hkl})^2]^{1/2}$, where I_p is the number of counts accumulated during the scan of the peak, I_{B_1} and I_{B_2} are the background counts on the low and high 2θ sides of the peak, S = scan speed in deg min^{-1} , R is the ratio of total background counting

time to scan time, $p = 0.02$ and $I_{hkl} = S[I_p - 1/R(I_{B_1} + I_{B_2})]$.

Wilson statistics indicated a centrosymmetric space group and the structure was solved in $Pbam$ from an interpretation of a three-dimensional Patterson map. The iron, oxygen and boron positions, the latter two determined from electron density maps, were refined by least squares. Using anisotropic thermal parameters and an extinction correction $g = 8 \times 10^{-6}$ the structure converted quickly to $R = 0.030$, $\omega R = 0.027$ for the 461 observed structure amplitudes. For the 614 measured $F(hkl)$ $R = 0.054$, $\omega R = 0.029$. Values of the scattering factors for neutral atoms corrected for the real and imaginary parts of dispersion were taken from *International Tables for X-ray Crystallography* (1974). The final difference electron density map showed only random variations of $\pm 0.8 \text{ e}\text{\AA}^{-3}$. The atomic parameters are shown in Table 1 and structure amplitudes in Table 2.¹

Discussion of structure

In Table 3 are shown the atomic bond distances of interest in this structure. The B–O distances in the triangular borate ion are in excellent agreement with those found in recent determinations of borate structures (Moore *et al.*, 1976; Konnert *et al.*, 1976). Figure 1 shows the (001) projection and it is unchanged from the previous descriptions (Takéuchi *et al.*, 1950; Takéuchi, 1956). The four crystallographically independent octahedra can be divided into two pairs which have nearly identical configurations. Labeling the octahedra by the iron occupant, Fe1 and Fe3 are similar and Fe2 and Fe4 are similar. In particular, the latter two have the 6 Fe–O distances nearly the same, while the former pair has distinctly longer Fe–O

¹ To receive a copy of Table 2, order Document AM-83-229 from the Business Office, Mineralogical Society of America, 2000 Florida Avenue, N.W. Washington D.C. 20009. Please remit \$1.00 in advance for the microfiche.

distances in the equatorial section. It strongly suggests that the four crystallographically independent Fe may be divided into two distinct pairs.

The formal valence balance based on the formula $2\text{FeO} \cdot \text{FeBO}_3$ requires two divalent and one trivalent iron ions. We calculated the valence sum for the crystallographic irons using the expressions $S = 1/3 (R/2.155)^{-5.5}$ for Fe^{2+} or $S = 1/2 (R/2.012)^{-5.3}$ for Fe^{3+} where S is the bond strength in valence units and R is the interatomic distance (Brown and Shannon, 1973), and found valence sums: $\text{Fe1} = 2.13$, $\text{Fe2} = 2.40$, $\text{Fe3} = 2.15$ and $\text{Fe4} = 2.63$. For B the valence sum was 2.97. The ions Fe1 and Fe3 are essentially divalent and Fe2 and Fe4 have intermediate valence. The long Fe–O bonds in the Fe1 and Fe3 octahedra are due to the extra electron in the t_{2g} manifold of high spin Fe^{2+} , probably in the d_{xy} orbital so that electrostatic repulsion lengthens this bond and produces a squashed octahedron (Johnson, 1971). The Fe2–Fe4 distance is 2.787\AA , considerably shorter than all other Fe–Fe distances in this structure. It is well established that an Fe–Fe distance of less than 3\AA can give rise to direct electronic exchange phenomena leading to an average valence for Fe2 and Fe4 (Goodenough, 1965).

Mössbauer spectroscopy

Experimental

Pure vonsenite suitable for Mössbauer study was obtained from the impure reaction mixture by washing the

mixture several times with 3M HNO_3 to dissolve the excess iron and then washing with distilled water to remove any remaining acid. X-ray diffraction powder patterns of the washed material had only lines from vonsenite. Mössbauer absorbers were prepared by mixing hand ground vonsenite with a small amount of vacuum grease. This mixture was spread evenly over a plastic film mounted on a 19 mm diameter aluminum ring to give an Fe concentration of about 20 mg/cm^2 . X-ray diffraction powder patterns of the prepared absorbers showed no evidence of preferred orientation.

Mössbauer spectra were obtained with an Austin Science Associates model 53 constant acceleration drive operated in the time mode. Data were accumulated in a Southwest Technical Products 6800 minicomputer until the total counts/channel exceeded 1 million counts. The source was 100 mCi of Co^{57} diffused into a Rh foil and was used at room temperature. Velocity calibration was obtained by laser interferometry (Cosgrove *et al.*, 1971). Low temperature spectra were obtained using an Air Products Displex model CS-202 closed cycle refrigeration system. Temperature control was accomplished by comparing the output voltage of a calibrated silicon diode to a reference voltage and using the result to cycle the refrigerator. Data collection was interrupted when the refrigerator was in operation.

Spectra were fitted using a program written by Stone *et al.* (1971) which fits a sum of Lorentzians using the Gauss nonlinear method. A value of 0.126 mm/sec was added to all peak positions in order to correct for source shift due to the rhodium matrix and reference the results to metallic iron.

Discussion

In Figure 2 the observed and calculated spectra are shown. The fitting procedure is based on five environments. The lowest velocity absorption band, which is a composite of five overlapping lines, was fit by only three lines. The resultant envelope for the complete spectrum fits the experimental points closely. Line 1 is paired with lines 4, 5 and 6. Lines 2 and 3 are paired with 8 and 7 respectively. After constraining the respective areas of lines 2 and 3 to be equal to the areas of lines 8 and 7, the area remaining in the low velocity envelope was not equal to the sum of the areas for lines 4, 5 and 6. At room temperature the area is approximately one half of the sum of the three areas and at lower temperatures it is about $1/3$ of the area. Table 4 contains the parameters which were used. A striking feature seen in the sequence of spectra as a function of temperature is the movement of a low velocity peak towards higher velocity as the temperature decreases. The fixed features in the spectra, lines 2–8 and 3–7, can be ascribed to the presence of two crystallographically independent divalent ions, Fe1 and Fe3. The former is in a crystallographically two-fold position and the latter in a four-fold position and the areas of peaks 8 and 7 are very close to the expected ratio of 2:1. The

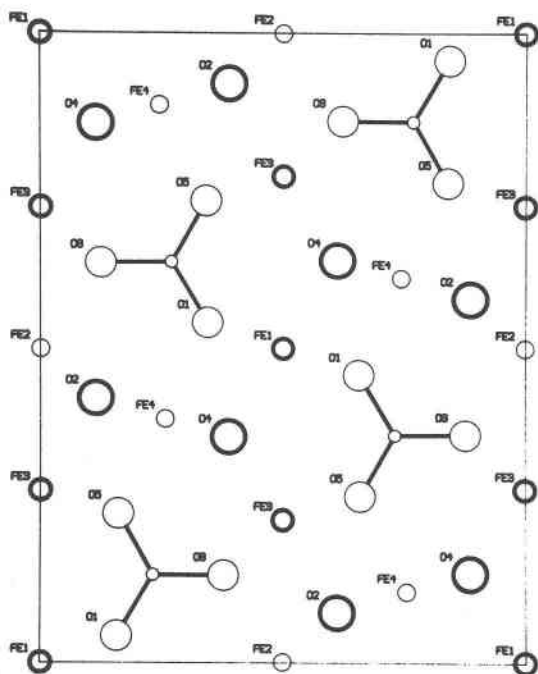


Fig. 1. Projection of vonsenite on (001). The smallest circle is B. The heavy circles are atoms at $z = 0$ and light circles at $z = 1/2$. The a axis is horizontal and b vertical.

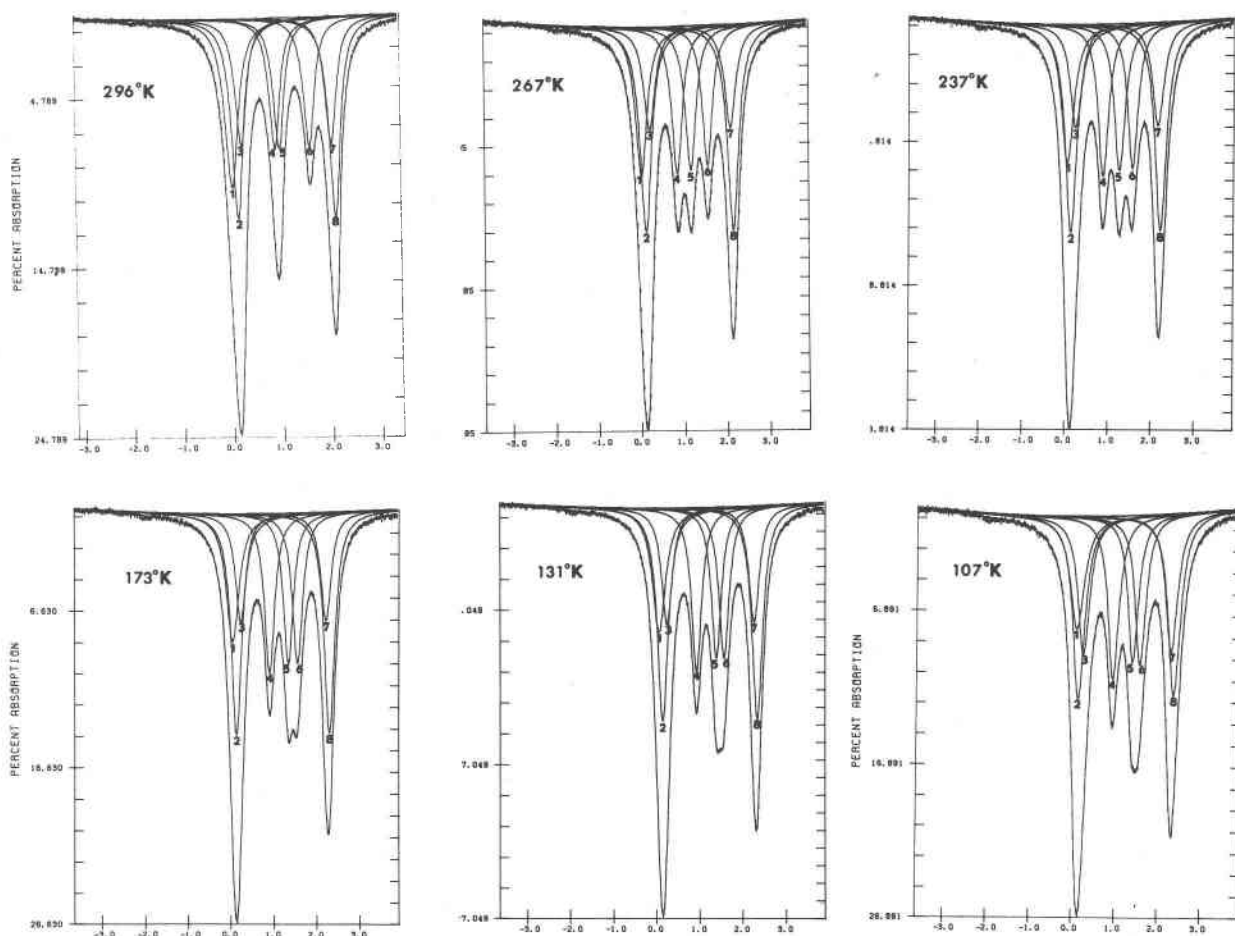


Fig. 2. Mössbauer spectra of vonsenite as a function of temperature. The horizontal axis is velocity in mm/sec.

parameters which fit line 4, and line 5 at room temperature, are characteristic of Fe^{3+} . The intermediate valence state characterized by the stationary line 6 must be ascribed to the presence in the crystal structure of charge transfer, electron delocalization, or perhaps to both pro-

cesses. Mixed valence states in minerals are frequently observed (Burns, 1981).

An examination of the iron-iron distances found in this structure, Table 3, shows very short Fe2-Fe4 distances of 2.787\AA and next nearest neighbor distances of 3.073\AA

Table 3. Bond distances (\AA) and angles ($^\circ$) in $2\text{FeO} \cdot \text{FeBO}_3$

| | | | | | | | |
|----------|------------|-----------|------------|---------|----------|-----------|------------|
| *4Fe1-01 | **2.200(1) | 04-Fe1-01 | 98.81(9) | Fe4-01 | 2.074(4) | 04-Fe4-04 | 99.89(6) |
| 2 -04 | 2.037(4) | 01-Fe1-01 | 91.37(4) | -05 | 2.071(5) | 04-Fe4-02 | 82.77(4) |
| 4Fe2-02 | 2.105(1) | 03-Fe2-02 | 95.46(10) | 2 -02 | 2.092(1) | 04-Fe4-02 | 177.23(6) |
| 2 -03 | 2.060(4) | 02-Fe2-02 | 93.79(5) | 2 -04 | 2.008(1) | 04-Fe4-01 | 85.06(11) |
| Fe3-02 | 2.102(4) | 03-Fe3-03 | 88.34(4) | Fe1-Fe1 | 3.073(1) | 04-Fe4-05 | 96.56(11) |
| -04 | 1.956(4) | 03-Fe3-02 | 81.10(9) | -Fe3 | 3.374(2) | 02-Fe4-02 | 94.57(5) |
| 2 -03 | 2.205(1) | 03-Fe3-05 | 88.75(4) | -Fe4 | 3.101(1) | 02-Fe4-01 | 94.42(10) |
| 2 -05 | 2.208(1) | 03-Fe3-05 | 161.45(12) | Fe2-Fe2 | 3.073(1) | 02-Fe4-05 | 83.87(10) |
| | | 03-Fe3-04 | 97.13(10) | -Fe3 | 3.176(1) | 01-Fe4-05 | 177.47(17) |
| | | 05-Fe3-05 | 88.21(5) | -Fe4 | 2.787(1) | | |
| | | 05-Fe3-04 | 101.41(8) | Fe3-Fe3 | 3.073(1) | | |
| | | 05-Fe3-02 | 80.34(9) | -Fe4 | 3.192(1) | | |
| | | 04-Fe3-02 | 177.52(16) | Fe4-Fe4 | 3.073(1) | | |
| | | | | B-01 | 1.387(8) | | |
| | | | | B-03 | 1.378(8) | | |
| | | | | B-05 | 1.380(8) | | |

* Coefficients designate the number of equal bonds.

** Numbers in parentheses represent the standard deviation and refer to the last decimal place.

Table 4. Mössbauer parameters of vonsenite as a function of temperature

| Peaks | | 296°K | 267°K | 237°K | 212°K | 173°K | 131°K | 107°K |
|-------|------------|-----------|-----------|-----------|-----------|-----------|-----------|-----------|
| 1-4 | IS* | 0.448(2) | 0.435(1) | 0.446(2) | 0.452(3) | 0.458(2) | 0.476(2) | 0.500(6) |
| | Q | 0.874(2) | 0.834(1) | 0.832(2) | 0.836(3) | 0.860(2) | 0.869(2) | 0.851(6) |
| | Γ | 0.260(2) | 0.296(2) | 0.294(2) | 0.296(2) | 0.283(2) | 0.282(2) | 0.306(2) |
| | A | 0.178(1) | 0.193(2) | 0.193(1) | 0.194(1) | 0.200(1) | 0.200(1) | 0.202(1) |
| 1-5 | IS | 0.491(2) | 0.592(1) | 0.636(2) | 0.658(3) | 0.678(2) | 0.704(2) | 0.730(6) |
| | Q | 0.961(2) | 1.150(1) | 1.214(2) | 1.246(3) | 1.299(2) | 1.327(2) | 1.311(6) |
| | Γ | 0.260(2) | 0.301(2) | 0.306(3) | 0.309(4) | 0.276(4) | 0.276(4) | 0.300(2) |
| | A | 0.178(1) | 0.193(2) | 0.194(2) | 0.195(3) | 0.184(4) | 0.182(5) | 0.180(1) |
| 1-6 | IS | 0.794(1) | 0.789(1) | 0.789(2) | 0.790(3) | 0.785(2) | 0.795(2) | 0.817(6) |
| | Q | 1.567(1) | 1.542(1) | 1.520(2) | 1.511(3) | 1.513(2) | 1.507(2) | 1.484(6) |
| | Γ | 0.269(2) | 0.281(2) | 0.286(2) | 0.289(3) | 0.284(3) | 0.284(3) | 0.300(2) |
| | A | 0.180(1) | 0.175(1) | 0.180(2) | 0.179(2) | 0.189(3) | 0.187(4) | 0.180(1) |
| 3-7 | IS | 1.111(4) | 1.151(3) | 1.178(5) | 1.189(5) | 1.211(4) | 1.238(4) | 1.257(7) |
| | Q | 1.816(4) | 1.878(3) | 1.918(5) | 1.968(5) | 1.986(4) | 2.029(4) | 2.052(7) |
| | Γ | 0.273(2) | 0.323(2) | 0.323(2) | 0.320(2) | 0.294(2) | 0.301(1) | 0.337(2) |
| | A | 0.180(9) | 0.147(1) | 0.143(9) | 0.169(12) | 0.141(7) | 0.152(8) | 0.188(10) |
| 2-8 | IS | 1.112(3) | 1.136(2) | 1.156(3) | 1.171(5) | 1.201(3) | 1.228(3) | 1.234(6) |
| | Q | 1.970(3) | 2.030(2) | 2.090(3) | 2.135(5) | 2.169(3) | 2.200(3) | 2.231(6) |
| | Γ | 0.273(2) | 0.323(2) | 0.323(2) | 0.320(2) | 0.294(2) | 0.301(1) | 0.337(2) |
| | A | 0.285(9) | 0.293(1) | 0.290(9) | 0.262(12) | 0.287(7) | 0.279(8) | 0.249(10) |
| | χ^2 | 1.462 | 1.474 | 1.960 | 1.841 | 1.351 | 1.422 | 1.861 |
| | MISFIT %** | 0.0027(5) | 0.0026(5) | 0.0053(6) | 0.0052(7) | 0.0025(6) | 0.0024(5) | 0.0058(7) |

* Isomer shift (IS), quadrupole splitting (Q), and line width (Γ) in mm/sec relative to metallic iron. A is fraction of total area for the high velocity peaks for each doublet. Standard deviations are in parentheses.

** MISFIT (Ruby, 1973).

parallel to the *c*-axis, between Fe2–Fe2 and Fe4–Fe4. The charge distribution based on stoichiometry should consist of divalent iron in the two-fold crystallographic sites occupied by Fe1 and Fe2 and the four-fold site occupied by Fe3; the four-fold trivalent site is labeled Fe4.

A trinuclear cluster formed by Fe4–Fe2–Fe4 is present in the structure with interatomic distances 2.878Å. This very short bond gives rise to orbital overlap and electron hopping occurs such that at a given instant one pair of iron ions has an intermediate valence state and one Fe4 is trivalent. This hopping mechanism is present at all temperatures and has a frequency less than 10^7 sec^{-1} . The very short iron–iron distance constitutes a deep potential well so that the residence time of the electron is relatively long. This model is consistent with the observation that the area of line 4 is representative of a crystallographically two-fold position and the parameters remain invariant with temperature. Also the parameters of line 6 are invariant over the temperature range investigated.

The 3.073Å distance parallel to the *c*-axis between Fe2–Fe2 and Fe4–Fe4 is nearly at the limit where direct exchange can take place (Goodenough, 1965). We postulate that at room temperature charge delocalization over the three-dimensional structure is present and line 5 is indicative of this situation. As the temperature decreases this relatively large iron–iron distance becomes a barrier and indeed this line moves from the low velocity absorption peak towards line 6 and nearly merges with it at 107 K to form a single peak with area indicative of a four-fold

site occupancy. Magnetic ordering takes place at 98 K and gives rise to a very complex Mössbauer spectrum.

Conclusion

X-ray structure results show that the four crystallographically independent Fe are grouped into two, physically distinct pairs. Fe1 and Fe3 are divalent and are surrounded by a squashed tetrahedron, while Fe2 and Fe4 have a very symmetric, octahedral environment and display intermediate valence of about 2.5. The observations that iron substituting for Mg^{2+} goes first into the M3 octahedron (Mokeyeva, 1968; Malisheva *et al.*, 1971), corresponding to the Fe2 octahedron in this paper, implies that the substituting Fe assumes an intermediate oxidation state rather than ferrous since the latter would preferentially go into an M2 (Fe1) octahedron. A more detailed picture of charge transfer and electron delocalization emerges from the temperature dependence of the Mössbauer spectra. The very short Fe–Fe distances of 2.787Å which exist in the trinuclear cluster formed by the edge sharing Fe4–Fe2–Fe4 octahedra permit strong direct overlap of iron *d* orbitals. Electron hopping occurs which at any instant produces one trivalent iron atom and one dinuclear cluster in which iron has an intermediate valence state. The two other crystallographically independent Fe1 and Fe3 are divalent in this compound. At room temperature a mechanism of charge delocalization over the complete structure is also operative. It is facilitated by the Fe2–Fe2 and Fe4–Fe4 distances of 3.073Å parallel to the *c*-axis. This intermetallic distance is at the very end

of the range where direct exchange is possible. As the temperature is lowered this path is inhibited and only charge transfer in a dinuclear cluster remains. This model predicts that a strong temperature dependence of electrical conductivity parallel to *c* should be observed in this material.

Acknowledgments

The authors are grateful for the support of the R. A. Welch Foundation of Houston, Texas. We thank Professor R. L. Collins of the Department of Physics, The University of Texas at Austin, for permission to use his Mössbauer apparatus.

References

- Bertaut, E. F. (1950) Structures of boroferrites. *Acta Crystallographica*, 3, 473–474.
- Brown, I. D. and Shannon, R. D. (1973) Empirical bond-strength–bond-length curves for oxides. *Acta Crystallographica*, A29, 266–282.
- Burns, R. G. (1981) Intervallence transitions in mixed valence minerals of iron and titanium. *Annual Review of Earth and Planetary Science*, 9, 345–383.
- Carvalho da Silva, J., Clark, J. R. and Christ, C. L. (1955) Crystal structure of ludwigite. (abstr.) *Geological Society of America Bulletin*, 66, 1540–1541.
- Cosgrove, J. G. and Collins, R. L. (1971) *Nuclear Instruments and Methods*, 95(2), 269.
- Eakle, A. S. (1920) Vonsenite, a preliminary note on a new mineral. *American Mineralogist*, 5, 141–143.
- Franz, G., Ackermann, D. and Koch, E. (1981) Karlite, $Mg_7(BO_3)_3(OH, Cl)_5$ a new borate mineral and associated ludwigite from the Eastern Alps. *American Mineralogist*, 66, 872–877.
- Goodenough, J. (1965) *Magnetism and the Chemical Bond*. Interscience Publishers, New York-London.
- International Tables for X-Ray Crystallography, vol. IV (1974) The Kynoch Press, Birmingham, England.
- Johnson, C. E. (1971) Structural problems in solid state chemistry. In I. Dezsi, Ed., *Proceedings of the Conference on the Application of the Mössbauer Effect* (Tihany, 1969), p. 663–679. Akademie Kiado, Budapest, Hungary.
- Konnert, J. A., Appleman, D. E., Clark, J. R., Finger, L. W., Kato, T., and Miura, Y. (1976) Crystal structure and cation distribution of hulsite, a tin–iron borate. *American Mineralogist*, 61, 116–122.
- Leonard, B. F. and Vlisidis, A. (1960) Vonsenite from St. Lawrence county, northwest Adirondacks, New York. *American Mineralogist*, 45, 439–442.
- Leonard, B. F. and Vlisidis, A. (1961) Vonsenite at the Jayville magnetite deposit, St. Lawrence county, New York. *American Mineralogist*, 46, 786–811.
- Malisheva, T. V., Yermakov, A. N., Alexandrov, S. M., and Kurash, V. V. (1971) Mössbauer study of isomorphism in borates of ludwigite and vonsenite series. In I. Dezsi, Ed., *Proceedings of the Conference on the Application of the Mössbauer Effect* (Tihany, 1969), p. 745–750. Akademie Kiado, Budapest, Hungary.
- Mokeyeva, V. I. (1968) Refinement of the structure of ludwigite ($Mg_{1.85}Fe_{0.15}^{2+}(Fe_{0.60}^{3+}Al_{0.40})BO_3O_2$ and the distributions of Mg^{2+} and Fe^{2+} in cation sites. *Geokhimiya*, 8, 975–979. (*Geochemistry International* (1968) 5, 809–813. In English.)
- Moore, P. B. and Araki, T. (1976) Painite, $CaZrB(Al_9O_{18})$: Its crystal structure and relation to jeremejevitte, $B_5[\square_3Al_6(OH)_3O_{15}]$, and fluoborite, $B_3[Mg_9(F, OH)_9O_9]$. *American Mineralogist*, 61, 88–94.
- Ruby, S. L. (1973) Why misfit when you already have X^{2+} ? *Mössbauer Effect Methodology*, 8, 263–277.
- Ruiz, J. L. and Salvador, P. S. (1971) Chemical and crystallographic data for vonsenite from Burguillos del Cerro, Badajoz, Spain. *American Mineralogist*, 56, 2149–2151.
- Stone, A. J., Augard, H. J., and Fenger, J. (1971) MOSSPEC. Program for Resolving Mössbauer Spectra. Publications Danish Atomic Energy Commission RISO-M-1348.
- Takéuchi, Y., Watanabe, T., and Ito, T. (1950) The crystal structures of warwickite, ludwigite and pinakiolite. *Acta Crystallographica*, 3, 98–107.
- Takéuchi, Y. (1956) The crystal structure of vonsenite. *Mineralogical Journal* (Mineralogical Society of Japan), 2, 19–26.

*Manuscript received, May 6, 1982;
accepted for publication, January 17, 1983.*